ELSEVIER

Diamond and Related Materials 10 (2001) 889–894

DIAMOND AND RELATED MATERIALS

www.elsevier.com/locate/diamond

Field emission studies of low-temperature thermal annealing of nitrogen-doped hydrogenated amorphous carbon (a-C:H:N) films

M.T. Kuo*, P.W. May, M.N.R. Ashfold

School of Chemistry, University of Bristol, Cantock's Close, Bristol BS8 1TS, UK

Abstract

Nitrogen-doped hydrogenated amorphous carbon (a-C:H:N) films have been deposited by radio frequency plasma methods using N_2/CH_4 gas mixtures. The effects upon optical and electronic properties of these films of low temperature (100–450°C) annealing in vacuum ($\leq 1 \times 10^{-5}$ torr) for various times were then studied. Such annealing causes a decrease in film thickness, probably due to evolution of species from the films, which is a function of annealing temperature and time. Laser Raman measurements show structural changes at 200°C. Fourier transform infra-red spectra indicate no change in CH bonding below temperatures of 450°C. Field emission results show that suitable post-treatment annealing at 200°C can reduce both the threshold field density and the threshold field by a factor of two. Annealed films also show an order of magnitude improvement in emission current for a given threshold field density. We also find an increase in the gradient of current–electric field curves, which extend to higher electric field values with increasing duration of annealing and with temperature.

Keywords: Field emission; Nitrogen doping; Amorphous carbon; Thermal annealing

1. Introduction

It has been reported that both the conductivity and electronic performance of hydrogenated amorphous carbon (a-C:H) films can be greatly improved by incorporation of nitrogen [1,2]. As a result, there have been a number of reports [3–5] describing attempts to nitrogenate a-C:H films by the addition of nitrogen-containing gases into the process gas mixture. Although low thermal stability is one of the main disadvantages of a-C:H films, thermal treatment can be used to modify the electrical properties of these films. However, the effects of annealing on the field emission efficiency are still not understood. Modifications of the defect distribution and microstructure in a-C:H films by vacuum annealing at high temperature have been attributed to a loss of hydrogen, and also to graphitisation [6]. Annealing CVD diamond at high temperature gives similar results [7–9], and it has been observed that the resistivity of CVD diamond films increases after annealing in vacuum or a N_2 atmosphere at temperatures of 350–800°C [10–12]. Previous attempts to produce n-type a-C:H films using nitrogen or phosphorus dopants deduced that the dopant species were in electronically inactive forms, even at high incorporation levels [13].

Work on undoped amorphous carbon and diamond-like carbon (DLC) films [14–16] showed that annealing can have a significant effect on many aspects of the film composition, structure and properties. One effect of

* Corresponding author. Fax: +44-870-126-9718.
E-mail address: mt.kuo@ms11.url.com.tw (M.T. Kuo).

0925-9635/01/$ - see front matter
PII: S0925-9635(00)00427-1

temperature is to cause species within the film to diffuse throughout the bulk, eventually reaching the film surface, where they may evaporate. The diffusion rates will be temperature-dependent, and will also depend upon the nature of the species. However, in order for species to be mobile, the available thermal energy must be greater than the activation energy trapping the species in the film. Interstitial species, or species which are non-bonded (such as N_2 molecules), can have very low activation barriers and may diffuse out of the bulk at low temperatures. With increasing temperature, it is possible to break chemical bonds, causing other species, such as H_2, CH_4 or other hydrocarbons, to desorb and finally evaporate. Diffusion of these species through the film is believed to occur via porous channels within the structure [10], and the size of the pores can determine the diffusion rate of different species. Annealing the film also affects the pore size, both in the bulk and on the surface of the film. If surface pores decrease in size on sample heating, it is possible that material from inside the bulk, especially larger hydrocarbons, will no longer be able to escape from the surface. This so-called 'skin effect' [17] is known to occur when annealing at high temperatures. The loss of species by evaporation causes the film to shrink, but it can also undergo structural modification. In particular, at higher temperatures, reactive sites (dangling bonds) can be created within the film as bonds are broken, and these can cross-link, altering the physical and electronic structure of the remaining film [18,19]. Another effect of thermal annealing is the modification of the film/substrate interface. Friedmann et al. reported that annealing of ta-C films at 600°C resulted in an improvement in adhesion [20]. Such a change might also affect field emission characteristics, since it is thought [21,22] that the emitted electrons may originate from this interfacial layer.

For doped films, yet more possibilities arise, since thermal annealing could 'activate' the films and turn the dopant into an electronically active form, without the drawbacks of delamination from increasing internal stress, or oxidation. In this work, we have investigated the effect of annealing on the observed film thickness, IR/Raman spectra and optical bandgap of a-C:H:N films. Furthermore, the effects on field emission are presented and the role of annealing in field emission properties is discussed.

2. Experimental

2.1. Film production

Film deposition was carried out in a conventional 13.56-MHz radio frequency parallel-plate reactor. Nitrogen-containing amorphous carbon (a-C:H:N) films were deposited using CH_4 and N_2 mixtures with flow rates of 10 sccm each. The reaction chamber was kept at a pressure of 20 mtorr and a DC bias of -80 V. Undoped films were deposited using the same conditions, but with no added nitrogen. Deposition lasted for either 30 min or 1 h, and the substrates were boron-doped Si(100) or quartz. After deposition, the films were transferred to a vacuum vessel containing silica gel, to minimise contamination or water adsorption, prior to treating and testing.

Table 1
Cooling rates obtained from a linear line of plots of ln(temperature, T) vs. time, t, for various annealing temperatures, and expressed by the equation $T = Ae^{kt}$

Annealing temperature (°C)	A (°C)	k (min^{-1})
100	93.0	−0.0097
150	148.6	−0.0149
300	289.0	−0.0155
400	380.9	−0.0168

2.2. Thermal processing

Samples were placed in a quartz tube and isothermally annealed in vacuum ($\leq 1 \times 10^{-5}$ torr) evacuated by a turbomolecular pump. The quartz tube was baked at temperatures ranging from 100 to 450°C in a preheated furnace for 30 min–48 h. The films were then gradually cooled back to room temperature in vacuum for $\sim$2.5–5 h. Cooling curves obeyed a linear relationship when plotted as ln(temperature) versus time. Cooling rates were obtained from a linear trend-line of curves with various annealing temperatures, and expressed as the equation $T = Ae^{kt}$ (see Table 1).

2.3. Film characterisation

Field emission testing was performed using a probe in a high vacuum chamber at 10^{-7} torr, which has been described in detail previously [23]. The thickness of films was obtained from cross-sectional scanning electron microscopy (SEM). The film structure was examined by laser Raman spectroscopy using a Renishaw 2000 spectrometer (325-nm laser excitation). Fourier transform infra-red (FTIR) absorption spectroscopy was also used to monitor changes in bonding, and UV-visible absorption spectroscopy allowed the optical bandgap to be determined by the Tauc plot [24].

3. Results and discussion

General observations are that, with increase in an-

nealing temperature, the structure becomes more graphitic, as observed for ta-C:H films by Conway et al. [25]. It was also found that annealed films are not only harder and more difficult to scratch than as-deposited films, but also have better adhesion onto the substrates. This could be due to the extent of the void structure, or an increase in the ratio of sp^3/sp^2 bonding that affects the mechanical properties of a-C:H films [14].

The nitrogen-doped films, deposited on quartz substrates at a DC bias of -80 V for 1 h, were examined using FTIR and UV-visible spectroscopy. Several maxima characteristic of $-CH_x$ stretching vibrations were identified in the IR spectra, with peaks centred at 2950, 2923 and 2868 cm^{-1}. Previous work [13] has shown that incorporation of nitrogen leads to a chemical shift and a reduction in intensity of these peaks. Compared to as-deposited films, IR spectra of films annealed at 200°C for 24 h show no distinct difference in intensity, position or total integrated areas of these peaks. This suggests no significant change in the total amount of IR-active hydrogen in CH bonds under these annealing conditions. In other words, annealing does not cause the loss of bound terminated hydrogen from the films, although H may still be lost from bridge sites or as molecular hydrogen. This is consistent with optical bandgap measurements, which show only small changes of $\sim 2\%$ from the initial values of approximately 3.05 eV. UV-visible absorption results show that, compared to undoped films, nitrogen-doped films have higher relative intensities of UV absorption. In addition, it was also observed that annealing of nitrogen-doped films results in an increase in the intensity of the UV absorption peak, which is contrary to the results seen with undoped films. A possible reason could be the removal of nitrogen, leading to an increase in the UV transparency.

Fig. 1 shows laser Raman spectra taken from as-deposited films and films annealed at 200°C for 24 h. For nitrogen-doped films, the graphitic G band (~ 1586 cm^{-1}) is barely evident, and structural changes within the film due to annealing are revealed by an increase in G band intensity, a shift of the G band to higher wavenumber, and a reduced FWHM. In contrast, for undoped films annealing causes no significant change in the Raman spectrum. It is also evident that the incorporation of nitrogen increases the D band intensity (centred at ~ 1355 cm^{-1}) and is associated with a decrease in the G band. Furthermore, annealing of nitrogen-doped films obviously increases the intensities of both the G and D bands. This might be evidence for the modification of doped films into a structure with greater long-range order. From the annealing of undoped films, and our recent work on microcombustion analysis [26], we believe that the significant structural modification is mainly due to the evolution of nitrogen-containing species, which were embedded in

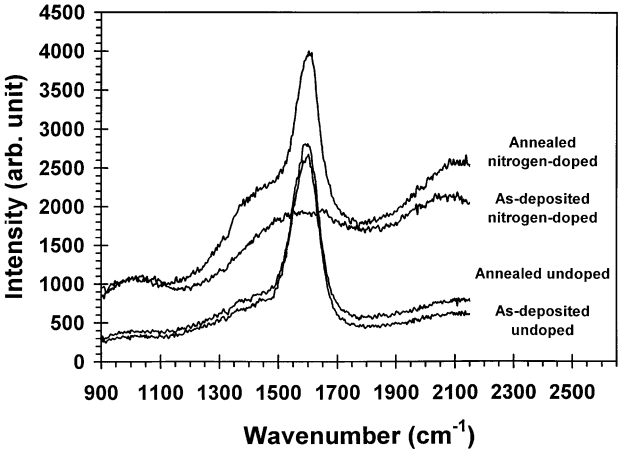

Fig. 1. Laser Raman spectra of undoped and nitrogen-doped amorphous carbon films deposited at a DC bias of -80 V for 1 h. Films were either as-deposited or annealed at 200°C for 24 h.

clusters, or intercalated within the matrix during deposition. The different behaviour of a-C:H films after annealing reported by Conway et al. [25] may be due to the different preparation methods [27].

Fig. 2 shows the variation of film thickness with varying temperature and annealing time, and the actual film thickness data are also given in Table 2. It can be seen that film thickness decreases with increasing annealing time. For films deposited on quartz substrates, a change of colour was observed, which was directly related to the change of film thickness. As Fig. 2 shows, higher temperatures produce a higher film shrinkage rate, presumably reflecting a higher evaporation rate. This is true, except for films annealed at very low temperatures (100°C) which show a dramatic decrease in thickness. This agrees with observations by Wächter et al. [28]. However, thermal desorption of bonded hydrogen and hydrocarbons is not found below threshold temperatures of 300–600°C [29,30], consistent with

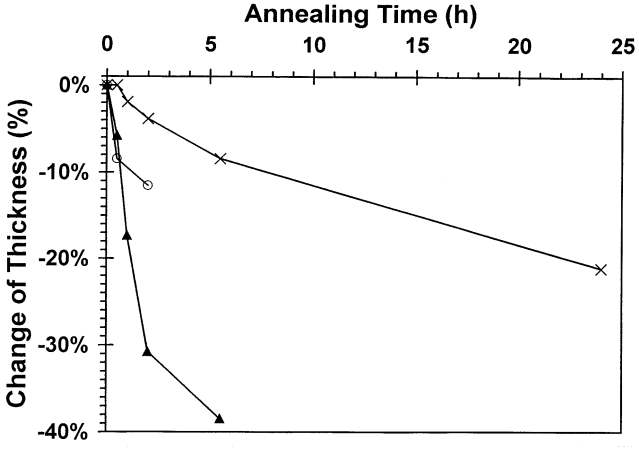

Fig. 2. Variation of film thickness with annealing time at temperatures of: (a) 100 (▲); (b) 200 (×); and (c) 450°C (○).

Table 2
Film thickness for various annealing temperatures as measured by cross-sectional SEM[a]

Annealing time (h)	Film thickness (μm)		
	100°C	200°C	450°C
0.5	0.49	0.52	0.48
1	0.43	0.51	N/A
2	0.36	0.50	0.46
5.5	0.32	0.48	
48		0.41	

[a]The film thickness of the as-deposited film was 0.52 μm.

the FTIR results above. The reason for this behaviour is not known, but the 'skin effect' (mentioned earlier), and/or a general decrease in pore size throughout the bulk on heating, could provide an explanation. At 100°C, there would be only a minor skin effect, and so trapped non-bonded species would readily diffuse out of the pores for long periods of time. At high temperature, the reduced pore-size traps species in the bulk, so reducing the evaporation rate. Another possibility is a closer packed arrangement of the pore structure, due to a much lower cooling rate for the 100°C annealing system (see Table 1).

Fig. 3 shows how the field emission characteristics of the films vary with the temperature and duration of annealing. Our previous work [13,23], and observations of Forrest et al. [31], pointed out that the field emission properties of a-C:H and a-C:H:N films are sensitive to variation in film thickness. Accordingly, dividing the measured threshold field (V_{th}) by the film thickness (d) counteracts this effect. The 'threshold density' is thus defined as V_{th}/d in units of V μm^{-2}. For comparison, the inset in Fig. 3 displays the raw threshold field data, which illustrate that the average threshold fields decrease with annealing time. For the films annealed at 200°C, Fig. 3 shows a dramatic decrease in threshold field density for the first 30 min, then no further improvement with time. Annealing at 450°C also shows an improvement in threshold field density, but with a more gradual downward trend for the first 2 h, which continues to decrease with further annealing. In contrast, unlike at higher temperatures, the films annealed at 100°C show an initial increase in threshold field density for the first 2 h, and then level out. Such mild annealing should not affect hydrogen termination or migration on the a-C:H surface, which disagrees with the proposal of Robertson et al. [2,32]. However, it is consistent with the idea that annealing at low temperatures simply causes evaporation of non-bonded or interstitial components (most likely free molecules) that raise the threshold field density, since the apparent improvement in threshold field is actually due to film shrinkage. Moreover, at temperatures higher than the threshold temperatures for various evolving species, the rate limiting factor is the size of pores, whereas at low temperatures the rate limiting factors are thermal desorption and diffusion in the porous amorphous films. These ideas are consistent with the model mentioned above, relating the film thickness and emission efficiency.

Field emission data for films annealed for 2 and 5.5 h at different temperatures are shown in Fig. 4a,b, respectively. The curves show two distinct regions. An initial sharp onset of emission and rapid increase in current with applied electric field density is evident. We refer to this region as the 'first stage emission', and attribute it to unmoderated field emission from the surface or the film/substrate interface. At higher currents, the gradient of the emission vs. field density plot reduces to a lower value. This 'second stage emission' is attributed to space- and interface-charge effects limiting the current flow.

Fig. 4a suggests two apparent effects of annealing. First, annealing increases the emission current for a given applied field density. This is especially true at higher annealing temperatures (200°C) when the emission current has increased by an order of magnitude. Second, the gradient of 'first stage emission' has increased, indicating that the emission has a sharper 'turn-on'. However, there is no significant change in the gradient of second stage emission. These effects might have important consequences for using these films in devices, where precise turn-on/turn-off would be desirable. Fig. 4b reveals a third effect of annealing. It shows that increasing the duration of annealing to 5.5 h gives an extension of first stage emission by up to two orders of magnitude, implying that thermal annealing could reduce the space- and interface-charge ef-

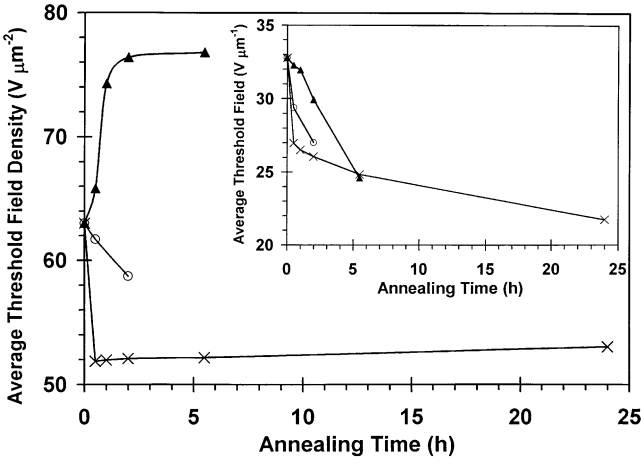

Fig. 3. Average threshold field density (defined as the threshold field in V μm^{-1} divided by the film thickness in μm) for a current of 10 nA as a function of annealing time at temperatures of: (a) 100 (▲); (b) 200 (×); and (c) 450°C (○). Inset: plots of average threshold field against annealing time for films annealed at the same three temperatures.

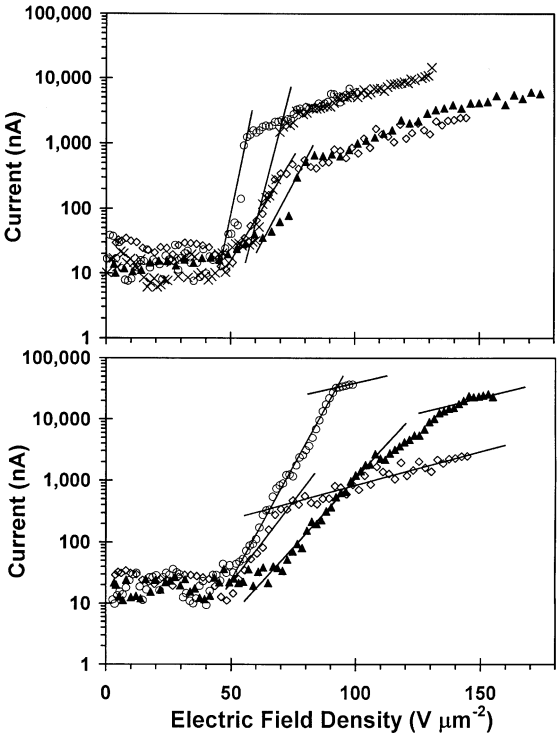

Fig. 4. Field emission characteristics of films. Emission current is plotted as a function of electric field density. In (a), annealing conditions are: (i) as-deposited (◇); (ii) 100°C, 2 h (▲); (iii) 200°C, 2 h (○); (iv) 450°C, 2 h (×). In (b), annealing conditions are: (i) as-deposited (◇); (ii) 100°C, 5.5 h (▲); and (iii) 200°C, 5.5 h (○). The gradients of first-stage and second-stage emission have been indicated by straight lines to guide the eye.

fects invoked to explain second stage emission, and thereby improve the field emission efficiency. However, the electric field density for the onset of emission threshold remains constant (~ 50 V μm^{-2}). According to the model of Xu et al. [33], our samples are located in the field region in which thermionic emission dominates with an interfacial barrier height of ~ 1.5 eV and an electrical field of $\sim 2.5 \times 10^7$ V m^{-1}. Thus, our films show a reasonable agreement with internal emission models [3,21,31].

4. Conclusion

The results presented above suggest that annealing of a-C:H:N films causes a number of effects, the combination of which lead to the observed results. An obvious effect is a decrease in film thickness resulting from the loss of film material. In general, this shrinkage is rapid at first, but after a short period, the rate of decrease slows. Closer inspection reveals that the effects of annealing seem to fall into three groups, determined by different temperature ranges.

For low temperatures (< 200°C), the thermal excitation is so low that probably only non-bonded or interstitial species (such as N_2 molecules) within the film are evolved. The remaining film does not reconstruct, but there could be an increase in pore density within the amorphous matrix [14], possibly leading to degradation of field emission properties. Moderate annealing temperatures (~ 200°C) provide sufficient energy to cause evaporation of both the non-bonded species and some weakly bound species. Removal of the latter will result in the creation of reactive sites (or dangling bonds) within the film, which can then cross-link, causing the film to become more ordered, as evidenced by increased G and D bands in Raman spectra. The structural rearrangement in the bulk might result in an increase in conductive pathways (e.g. ionised N donor centres [34]), and hence an improvement in field emission properties, both in terms of increased emission current and reduced threshold field. Finally, at high annealing temperatures (> 200°C), the available thermal energy is sufficient that components within the film can undergo a much greater variety of chemical reactions [29,30] associated with the evolution of hydrogen [18] or other species. Some strongly bonded species can now also overcome the activation barrier for evaporation, resulting in rapid loss of many more components of the film. However, the loss rate is not as dramatic as expected due to the skin effect, which reduces the conductance of pores. Field emission properties are somewhat improved, since the film will again undergo structural rearrangements similar to those mentioned above. Therefore, it appears that, in order to minimise field emission threshold density, annealing should be performed at a moderate temperature for approximately 1 h, but for maximum emission current (for a given applied potential), larger annealing times are beneficial.

Clearly, there is still a lot to be understood about the many effects of annealing on a-C:H:N films. In particular, the microstructural modifications of interface, bulk and surface need much further study.

Acknowledgements

M.T. Kuo would like to thank Mr G. Evans of Bristol University Physics Department for assistance with the Raman spectroscopy analysis.

References

[1] J. Schwan, W. Dworshak, K. Jung, H. Ehrhardt, Diamond Relat. Mater. 3 (1994) 1034.
[2] B.S. Satyanaryana, A. Hart, W.I. Miline, J. Robertson, Appl. Phys. Lett. 71 (1997) 1431.
[3] G.A.J. Amaratunga, S.R.P. Silva, Appl. Phys. Lett. 68 (1996) 2529.
[4] D.F. Franceschini, F.L. Freire, C.A. Achete, G. Mariotto, Diamond Relat. Mater. 5 (1996) 471.

[5] M.M. Lacerda, D.F. Franceschini, F.L. Friere, G. Mariotto, Diamond Relat. Mater. 6 (1997) 631.
[6] J.K. Walters, D.M. Fox, T.M. Burke, O.D. Weedon, R.J. Newport, W.S. Howells, J. Chem. Phys. 101 (1994) 4288.
[7] P.M. Fabis, Thin Solid Films 288 (1996) 193.
[8] R.S. Swineford, D.P. Pappas, V.G. Harris, Phys. Rev. B: Condens. Mater. 52 (1995) 7890.
[9] G. Davies, S.C. Lawson, A.T. Collins, A. Mainwood, S.J. Sharp, Phys. Rev. B: Condens. Mater. 46 (1992) 13157.
[10] I.M. Buckley-Golder, Diamond Relat. Mater. 1 (1991) 43.
[11] M.I. Landstrass, K.V. Ravi, Appl. Phys. Lett. 55 (1989) 975.
[12] S. Sahli, D.M. Aslam, Appl. Phys. Lett. 69 (1996) 2051.
[13] M.T. Kuo, P.W. May, A. Gunn, M.N.R. Ashfold, R.K. Wild, Diamond Relat. Mater. 9 (2000) 1222.
[14] X. Jiang, W. Beyer, K. Reichelt, J. Appl. Phys. 68 (1990) 1378.
[15] A. Grill, B. Meyerson, V. Patel, J.A. Reimer, M.A. Petrich, J. Appl. Phys. 61 (1987) 2874.
[16] A. Grill, V. Patel, B. Meyerson, in: Diamond and Diamond-Like Films and Coatings, Vol. 266. NATO-ASI Serial B: Physics, edited by R.E. Clausing, L.L. Horton, J.C. Angus and P. Kiodl. Plenum, New York, 1991. p. 417.
[17] C.N. Satterfield, Heterogeneous Catalysis in Practice, McGraw-Hill, New York, 1980, p. 114.
[18] D.R. Tallant, J.E. Parmeter, M.P. Siegal, R.L. Simpson, Diamond Relat. Mater. 4 (1995) 191.
[19] B. Dischler, A. Bubenzer, P. Koidl, Solid State Commun. 48 (1983) 105.
[20] T.A. Friedmann, J.P. Sullivan, J.A. Knapp et al., Appl. Phys. Lett. 71 (1997) 3820.
[21] P. Lerner, N.M. Miskovsky, P.H. Cutler, J. Vac. Sci Technol. B 16 (1998) 900.
[22] N. Koenigsfeld, B. Philosoph, R. Kalish, Diamond Relat. Mater. 9 (2000) 1218.
[23] M.T. Kuo, P.W. May, A. Gunn, J.C. Marshall, M.N.R. Ashfold, K.N. Rosser, Int. J. Mod. Phys. B 14 (2000) 295.
[24] J. Tauc, in: F. Abeles (Ed.), Optical Properties of Solids, North-Holland, Amsterdam, 1972, p. 270.
[25] N.M.J. Conway, A.C. Ferrari, A.J. Flewitt et al., Diamond Relat. Mater. 9 (2000) 765.
[26] M.T. Kuo, P.W. May, M.N.R. Ashfold, unpublished results.
[27] K.E. Spear, J.P. Dismukes, Synthetic Diamond: Emerging CVD Science and Technology, John Wiley & Sons, New York, 1994, p. 129.
[28] R. Wächter, A. Cordery, Diamond Relat. Mater. 8 (1999) 504.
[29] M. Malhotra, S. Kumar, Diamond Relat. Mater. 6 (1997) 1830.
[30] C. Wild, P. Koidl, Appl. Phys. Lett. 51 (1987) 1506.
[31] R.D. Forrest, A.P. Burden, S.R.P. Silva, L.K. Cheah, X. Shi, Appl. Phys. Lett. 73 (1998) 3784.
[32] J. Robertson, Proceedings of IVMC '98, (1998) 162.
[33] N.S. Xu, J. Chen, S.Z. Deng, Appl. Phys. Lett. 76 (2000) 2463.
[34] S.R.P. Silva, J. Robertson, G.A.J. Amaratunga et al., J. Appl. Phys. 81 (1997) 2626.